Time-Warping Based End-of-T-Wave Shape Marker Reflects Repolarization Changes During Ischemia

Neurys Gómez[1,2], Julia Ramírez[1,3,4], Juan Pablo Martínez[1,4], Pablo Laguna[1,4]

[1] BSICoS Group, I3A, IIS Aragon, University of Zaragoza, Zaragoza
[2] University of Oriente, Santiago de Cuba, Cuba
[3] William Harvey Research Institute, Queen Mary University of London, London, United Kingdom
[4] Centro de Investigación Biomédica en Red – BBN (CIBER-BBN), Zaragoza, Spain

Abstract

This work proposes to use a warping-based T-wave morphology index, d_w, estimated only in the T-wave peak-to-end interval, to capture ischemia-induced dispersion of repolarization, avoiding the influence of ST segment elevation/depression. ECG recordings acquired during elective balloon percutaneous coronary intervention (PCI) were analyzed, together with their baseline recordings. A d_w series was obtained by comparing the morphology of Mean Warped T wave peak-to end intervals (MWTPE) along the recordings with a reference MWTPE. A relative marker, $\mathcal{R}_d^{\text{PCA}}$, normalizing the d_w changes during PCI relative by the magnitude of the change during baseline recordings, was used to quantify the relative morphological variations generated by ischemia. d_w changes during PCI followed a well marked gradual increasing trend as inflation time progressed reaching at the occlusion end a median $\mathcal{R}_d^{\text{PCA}}$ value of 9.44 ms, (range from 1.01 to 80.74). During baseline recordings d_w remained stable with median $\mathcal{R}_d^{\text{PCA}}$ value of 1.00 ms, (range from 0.03 to 2.93 ms). Repolarization changes achieved $\mathcal{R}_d^{\text{PCA}} > 1, 2, 5, 10$ during PCI in 94.1%, 85.11%, 64.4% and 48.5% of patients, respectively, being significantly higher than its corresponding control recordings. In conclusion, the d_w marker is able to quantify ischemia-induced repolarization dispersion changes in a robust manner independent of the ST changes.

1. Introduction

Ischemic events result in an increased dispersion of ventricular repolarization, reflected at the T wave of the ECG, and known to be associated with increased arrhythmic risk [1]. In particular, several biomarkers have been previously proposed to assess ventricular arrhythmic risk, such as the QT interval [2], T-width [3], the distance from the peak to the end of the T-wave ($\mathrm{T_{pe}}$ interval) [4] or T-wave alternans [5]. Temporal reparametrization (warping) between two T-wave morphologies, using the d_w index, proposed by Ramírez et al. [6] allows to quantify variations in the overall morphology of the T-wave . This index has demonstrated to be more strongly associated with ventricular arrhythmias risk than the previously mentioned biomarkers.

The original formulation of the warping methodology for T wave analysis [6] includes warping of the complete T wave (from T-wave onset to T-wave end). However, ischemic conditions concur on the ECG with an elevation, or depression, of the ST segment as well as early phase T-wave changes, potentially influencing the correct measurement of the warping markers surrogates of ventricular repolarization dispersion. To avoid this interference in the repolarization dispersion significance of d_w, we hypothesized that d_w, estimated restrictively between the peak and end of the T wave, may better quantify the ischemia-induced dispersion of repolarization changes.

1.1. Materials and Methods

1.2. Data set

The study population included 101 patients (63 males and 38 females) from the STAFF III database [7] undergoing elective balloon percutaneous coronary intervention (PCI). ECG recordings were digitized at a sampling rate of 1000 Hz and an amplitude resolution of 0.625 μV. In this study we analyze two ECG recordings for each patient: the ECG recorded at rest during the 5 minutes previous to the catheter insertion (baseline recording) in supine position, and the ECG acquired during the first balloon inflation (PCI recordings). The spatial locations of the 101 balloon inflations were: left anterior descending (LAD) artery in 33 patients, left main (LM) artery in 2 patients, right coronary artery (RCA) in 45 patients and left circunflex artery (LCX) in 21 patients.

1.3. ECG Pre-processing

The ECG pre-processing included the following steps. First, the signal was low-pass filtered with a 40-Hz cut-off frequency sixth-order Butterworth filter to remove electric and muscle noise, and high-pass filtered with a 0.5-Hz cut-off frequency sixth-order Butterworth filter to remove baseline wander. Second, the QRS fiducial points were determined for each of the eight leads using a Wavelet-based single-lead method [8]. Then, a multi-lead selection rule strategy [9] was applied over the single-lead onsets and ends to obtain multilead QRS fiducial points. Third, spatial Principal Component Analysis (PCA) transformation, was applied to the eight independent leads, where the eigenvectors and eigenvalues were restrictively estimated from the T-wave samples. Fourth, the first principal component was further single-lead technique delineated with the obtained fiducial points used for the subsequent ECG analysis. Finally, each T-wave was further low-pass filtered at 20 Hz cut-off frequency with a sixth order Butterworth filter.

1.4. T-wave morphology changes quantification

At each record, T waves were extracted from each s-th 15 s duration window which moves sliding by 5 s resulting in 10 s windows overlap. For each s-th window, a mean warped T wave (MWTW) [6] restricted to the T-peak to T-end interval (MWTPE) was calculated, $\boldsymbol{f}^s(\boldsymbol{t}^s) = [f^s(t^s(1)), ..., f^s(t^s(N_s))]^T$, where $\boldsymbol{t}^s = [t^s(1), ..., t^s(N_s))]^T$. Initially, all T-waves within a given window were transformed to positive polarity waves. The predominant class between biphasic or monophasic T waves was defined for each window as the class having the highest number of occurrences. Only those T waves that were of the same class as the predominant one were considered to compute the MWTPE. Additionally, in order to avoid the effect of delineation errors, only T waves whose width T_w satisfies $T^s_{w,m} - 40 \leq T_w \leq T^s_{w,m} + 40$ (ms) were considered for the MWTPE estimation, where $T^s_{w,m}$ is the median of the T wave duration within each s-th window.

Warping functions and d_w series estimation: The MWTPE d_w estimation through each recording was perfomed using the method originally proposed by Ramírez *et al.* [6]. This method estimates the biomarker d_w as the mean amount of warping needed to minimise the time domain differences among two different waves, the one under study $\boldsymbol{f}^s(\boldsymbol{t}^s)$, and the reference $\boldsymbol{f}^r(\boldsymbol{t}^r)$. The reference MWTPE was estimated at the beginning of the recording in the baseline recording, and during the first seconds after balloon inflation in the PCI recordings. Fig. 1a. shows an example of the MWTPEs before time-warping, $\boldsymbol{f}^r(\boldsymbol{t}^r)$ calculated at the beginning of a PCI recording and $\boldsymbol{f}^s(\boldsymbol{t}^s)$ calculated at a window two minutes later.

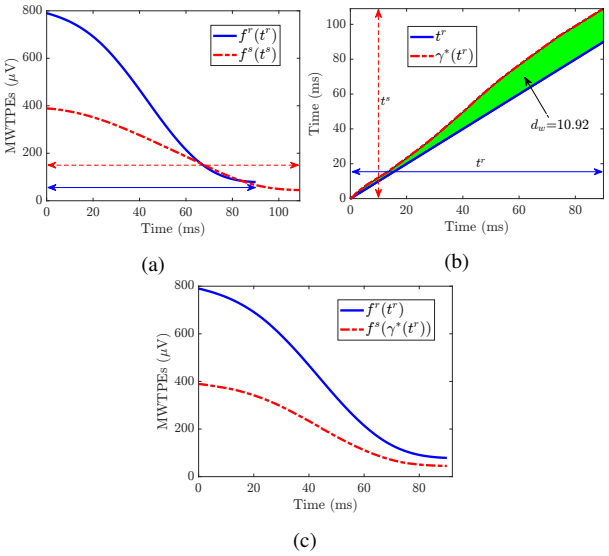

Figure 1: Stages of time-warping index extraction from two different waves from a particular patient. Panel (a) shows both the reference $\boldsymbol{f}^r(\boldsymbol{t}^r)$ (solid blue) and the s-th $\boldsymbol{f}^s(\boldsymbol{t}^s)$ (doted line red) original MWTPE. Panel (b) shows the warping function $\gamma^*(\boldsymbol{t}^r)$ (dotted line red) that optimally relates the reference and studied MWTPE. The area between $\gamma^*(\boldsymbol{t}^r)$ and $\boldsymbol{t}^r$ (green region) represents the total warping amount, quantified by d_w. Panel (c) shows the MWTPEs after warping $\boldsymbol{f}^s(\gamma(\boldsymbol{t}^r))$, dotted red line, together with the reference $\boldsymbol{f}^r(\boldsymbol{t}^r)$, in blue.

Let $\gamma(\boldsymbol{t}^r)$ be the warping function that relates $\boldsymbol{t}^r$ and $\boldsymbol{t}^s$ such as the composition $[\boldsymbol{f}^s \circ \gamma](\boldsymbol{t}^r) = \boldsymbol{f}^s(\gamma(\boldsymbol{t}^r))$ denotes the re-parameterization o time-warping of the $\boldsymbol{f}^s(\boldsymbol{t}^s)$ using $\gamma(\boldsymbol{t}^r)$. As in [6], the square-root slope function (SRSF) was used instead of the original signals, to find the optimal warping function so avoiding the so called "pinching effect". The SRSF is defined as the square-root of the derivative of $\boldsymbol{f}(\boldsymbol{t})$, considering the sign,

$$\boldsymbol{q}_f(\boldsymbol{t}) = sign\left(\dot{\boldsymbol{f}}(\boldsymbol{t})\right)\sqrt{|\dot{\boldsymbol{f}}(\boldsymbol{t})|}. \tag{1}$$

The optimal warping function, $\gamma^*(\boldsymbol{t}^r)$, is the one that minimizes the amplitude difference between the SRSF of $\boldsymbol{f}^r(\boldsymbol{t}^r)$ and $\boldsymbol{f}^s(\gamma(\boldsymbol{t}^r))$,

$$\gamma^*(\boldsymbol{t}^r) = \underset{\gamma(\boldsymbol{t}^r)}{\arg\min}\left(\|\boldsymbol{q}_{\boldsymbol{f}^r}(\boldsymbol{t}^r) - \boldsymbol{q}_{\boldsymbol{f}^s}(\gamma(\boldsymbol{t}^r))\sqrt{\dot{\gamma}(\boldsymbol{t}^r)}\|\right). \tag{2}$$

To solve this optimisation problem the dynamic programming algorithm was used [10]. The optimal warping function $\gamma^*(\boldsymbol{t}^r)$, that optimally relates $\boldsymbol{f}^s(\boldsymbol{t}^s)$ and $\boldsymbol{f}^r(\boldsymbol{t}^r)$ in Fig. 1a is shown in Fig. 1b. The warped T-wave, $\boldsymbol{f}^s(\gamma(\boldsymbol{t}^r))$, and the reference T-wave, $\boldsymbol{f}^r(\boldsymbol{t}^r)$, are shown in Fig. 1c.

The level of warping reflects information regarding the amount of time stretching required to fit the two waves, and

consequently the time domain difference between them. The d_w biomarker, quantifies this level of warping needed to optimally fit two T-waves as the average of the absolute difference value between $\gamma(\boldsymbol{t}^r)$ and $\boldsymbol{t}^r$:

$$d_w = \frac{1}{N_r}\sum_{n=1}^{N_r} |\gamma^*(\boldsymbol{t}^r(n)) - \boldsymbol{t}^r(n)| \tag{3}$$

This estimate of the d_w biomarker was repeated for each $\boldsymbol{f}^s(\boldsymbol{t}^s)$ MWTPE calculated for each s-th 15-second window to analyze its time course in induced-ischemia situations, resulting in a series $d_w^{\text{PCA}}(s)$ ($s \in \{1,\ldots,S\}$) every 5 seconds with respect to the initial stage taken at reference.

To analyze the warping value generated at any timing of the PCI intervention, we also use $\mathcal{R}_d$, defined similarly to the ischemic changes sensor proposed in [11], relative to the standard deviation of d_w at the baseline recording. In this work, $\mathcal{R}_d$ was defined as,

$$\mathcal{R}_d(s) = \frac{\Delta_d^{\text{PCI}}(s)}{\sigma_d^c}, \tag{4}$$

where $\Delta_d^{\text{PCI}}(s)$ is the magnitude of change in $d_w(s)$ during PCI occlusion at that timing denoted by s indexing. McNemar analysis is used for comparison between baseline and PCI recordings. A p value ≤ 0.05 was considered as statistically significant.

2. Results and discussion

An example of the temporal evolution of $d_w^{\text{PCA}}(s)$ for a particular patient in control and PCI is shown in Fig. 2a. The red trace represents the balloon inflation period, and different time instants (marked with letters) have been chosen to display the evolution of MWTPEs (Fig. 2b). Strong shape variations were observed, accompanied by $d_w^{\text{PCA}}(s)$ magnitude changes (ranging from 0.0 to 10.1 ms) following an increasing trend as inflation time progresses. On the contrary, $d_w^{\text{PCA}}(s)$ magnitude during baseline remained stationary with values ranging from 0.0 to 1.8 ms. No significant changes were observed in the control recording, whereas a decrease in amplitude and an increase in width of the $\boldsymbol{f}^s(\boldsymbol{t}^s)$ MWTPEs are observed in the inflation period, as reflected in the $d_w^{\text{PCA}}(s)$ trace in Fig. 2a.

The averages of $d_w^{\text{PCA}}(s)$, denoted as $\overline{d}_w^{\text{PCA}}(s)$, across all patients, aligned to the recording onset or to the balloon inflation onset, for baseline and PCI recordings, respectively, are shown in Fig. 3, (blue line). All records in the database were averaged. Dotted black line represents the number of recordings averaged in each timing. Note that the averages around the 5-th minute have little significance due to the available number of averaged records declining quickly at that timing, Fig. 3b. The time-course behavior of the d_w biomarker confirmed that it was able to sensibly capture the variations between the peak and end of the T wave, representing specifically the ischemia-induced dispersion of repolarization changes, avoiding ischemia-induced ST elevation/depression influence and early T waves changes.

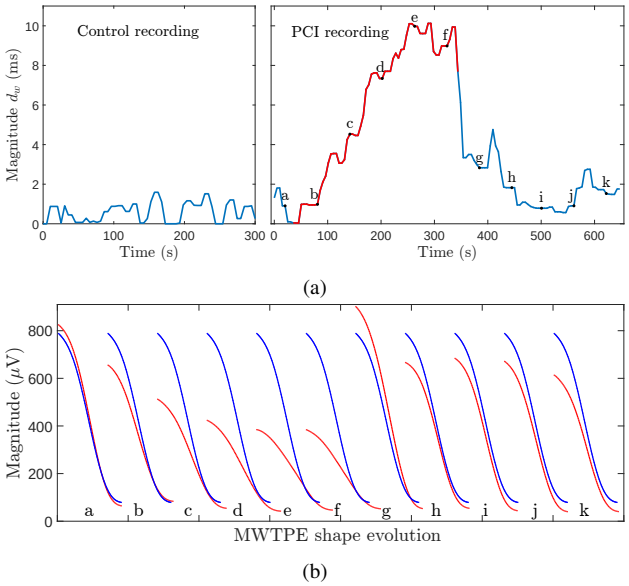

Figure 2: Time course of $d_w^{\text{PCA}}(s)$ along control and PCI recordings for a particular patient, together with T-wave from peak-to-end shape changes evolution. Changes evolution of $d_w^{\text{PCA}}(s)$ are shown in panel (a). Red line represents balloon inflation period. Panel (b) reflects the shape of the MWTPE (red dashed line) corresponding to the moments marked with letters in (a) together with the reference MWTPE (blue line).

The standard deviation in the control recording, σ_d^c had a median of 0.54 [IQR: 0.33], ranging from 0.02 to 2.08 ms. In order to test the stability of d_w in the control recording, $\mathcal{R}_d^{\text{PCA}}$ was also estimated in the second half of the baseline record relative to first half, showing a median value of 1.00 [IQR: 1.13], ranging from 0.03 to 2.93, while $\mathcal{R}_d^{\text{PCA}}$ magnitude at the end of the occlusion ranged from 1.01 to 80.74 (mean/median: 17.55/9.44). This suggest that in baseline conditions (without induced ischemic changes) they have small values just reflecting natural beat to beat ECG variability.

The analysis on the number of records during PCI stage where $\mathcal{R}_d^{\text{PCA}}$, evaluated as in (4) for $s = s^{\text{PCIend}}$, was larger than 1, 2, 5 and 10, were 94,1%, 85.11%, 64,4% and 48.5%, respectively. All percentages of PCI recordings were found significantly higher than in the control recordings: McNemar test $p = 3.7{\cdot}10^{-11}$, $4.0{\cdot}10^{-21}$, $5.4{\cdot}10^{-20}$ and $3.6 \cdot 10^{-15}$, for thresholds 1, 2, 5 and 10, respectively. The latter indicates that this marker can be used to quantify changes induced by ischemia on ventricular repolarization from changes from natural variability.

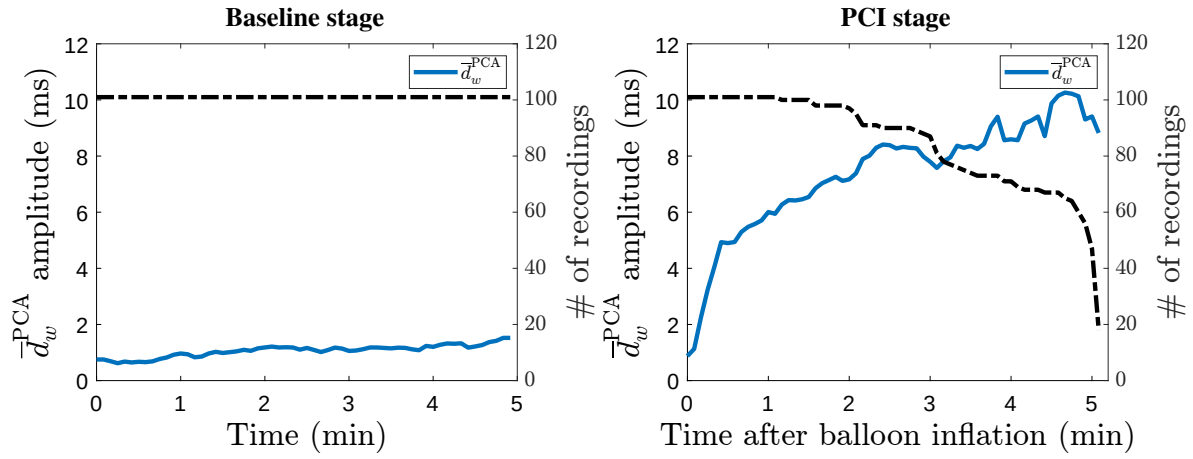

(a) (b)

Figure 3: Average over patients of the $d_w^{\text{PCA}}(s)$ time-course, $\overline{d}_w^{\text{PCA}}(s)$, (a) relative to the onset of the recording in control records and (b) aligned to the onset of the balloon inflation during PCI recording. Dotted black line shows the number of averaged recordings.

3. Conclusions

The T wave time-warping shape marker, d_w, restricted to T-peak to T-end interval, allows to capture ischemia-induced repolarization dispersion changes as reflected by the morphology changes of $\mathrm{T_{pe}}$ interval, potentially enabling its use as a biomarker in future arrhythmia risk estimation studies.

Acknowledgments

This work was funded by projects PID2019-104881RB-I00 and PID2019-105674RB-I00 by Spanish MICINN and FEDER, and by Gobierno de Aragon, BSICoS Group T39-20R, cofunded by FEDER 2014-2020 “Building Europe from Aragon”. JR acknowledges funding from the European Union-NextGenerationEU.

References

[1] Ramírez J, van Duijvenboden S, Aung N, Laguna P, Pueyo E, Tinker A, Lambiase PD, Orini M, Munroe PB. Cardiovascular predictive value and genetic basis of ventricular repolarization dynamics. Circulation Arrhythmia and Electrophysiology 2019;12(10):e007549.

[2] Moss AJ. Measurement of the QT interval and the risk associated with QTc interval prolongation: a review. The American journal of cardiology 1993;72(6):B23–B25.

[3] Fuller MS, Sandor G, Punske B, Taccardi B, MacLeod RS, Ershler PR, Green LS, Lux RL. Estimates of repolarization dispersion from electrocardiographic measurements. Circulation 2000;102(6):685–691.

[4] Azarov JE, Demidova MM, Koul S, Van Der Pals J, Erlinge D, Platonov PG. Progressive increase of the T peak - T end interval is associated with ischaemia-induced ventricular fibrillation in a porcine myocardial infarction model. EP Europace 2018;20(5):880–886.

[5] Narayan SM. T-wave alternans and the susceptibility to ventricular arrhythmias. Journal of the American College of Cardiology 2006;47(2):269–281.

[6] Ramirez J, Orini M, Tucker JD, Pueyo E, Laguna P. Variability of ventricular repolarization dispersion quantified by time-warping the morphology of the T-waves. IEEE Transactions on Biomedical Engineering 2016;64(7):1619–1630.

[7] Martínez JP, Pahlm O, Ringborn M, Warren S, Laguna P, Sörnmo L. The STAFF III database: ECGs recorded during acutely induced myocardial ischemia. In 2017 Computing in Cardiology (CinC). IEEE, 2017; 1–4.

[8] Martínez JP, Almeida R, Olmos S, Rocha AP, Laguna P. A wavelet-based ECG delineator: evaluation on standard databases. IEEE Transactions on biomedical engineering 2004;51(4):570–581.

[9] Laguna P, Jané R, Caminal P. Automatic detection of wave boundaries in multilead ECG signals: Validation with the CSE database. Computers and biomedical research 1994; 27(1):45–60.

[10] Bertsekas DP. Dynamic programming and optimal control. belmont. MA Athena Scientific 2000;.

[11] Garcıa J, Lander P, Sörnmo L, Olmos S, Wagner G, Laguna P. Comparative study of local and Karhunen–Loève-based ST-T indexes in recordings from human subjects with induced myocardial ischemia. Computers and Biomedical Research 1998;31(4):271–292.

Address for correspondence:

Neurys Gómez Fonseca, Campus Río Ebro, I+D Building, D-5.01.1B, C. Mariano Esquillor, s/n, 50018 Zaragoza (Spain)
794826@unizar.es